Society for Endocrinology
JOURNAL OF ENDOCRINOLOGY

Prenatal androgen exposure affects ovarian lipid metabolism and steroid biosynthesis in rats

Journal:	*Journal of Endocrinology*
Manuscript ID	JOE-20-0304.R2
Manuscript Type:	Research Paper
Date Submitted by the Author:	n/a
Complete List of Authors:	Abruzzese, Giselle Adriana; CEFYBO, Laboratorio de Fisio-patologia Ovarica Heber, Maria Florencia; CEFYBO, Laboratorio de Fisio-patologia Ovarica Ferreira, Silvana Rocio; Centro de Estudios Farmacologicos y Botanicos, Laboratorio de Fisio-patologia Ovarica; Centro de Estudios Farmacológicos y Botánicos, Ferrer, Maria José; Centro de Estudios Farmacologicos y Botanicos, Laboratorio de Fisiopatología ovárica Motta, Alicia Beatriz; CEFYBO, Laboratorio de Fisio-patologia Ovarica
Keywords:	developmental programming, Ovary, androgen excess, Steroidogenesis, Cholesterol

Prenatal androgen exposure affects ovarian lipid metabolism and steroid biosynthesis in rats

Giselle Adriana Abruzzese[1*], Maria Florencia Heber[1], Silvana Rocío Ferreira[1], María José Ferrer[1], Alicia Beatriz Motta[1]

[1]Laboratorio de Fisio-Patología Ovárica, Centro de Estudios Farmacológicos y Botánicos (CEFYBO), Consejo Nacional de Investigaciones Científicas y Técnicas (CONICET), Facultad de Medicina, Universidad de Buenos Aires (UBA), Argentina.

*Corresponding Author: Giselle A. Abruzzese - Laboratorio de Fisio-Patología Ovárica, Centro de Estudios Farmacológicos y Botánicos (CEFYBO), Consejo Nacional de Investigaciones Científicas y Técnicas (CONICET), Facultad de Medicina, Universidad de Buenos Aires (UBA) Paraguay 2155, Buenos Aires, Argentina, C1121ABG. Telephone: +54 11 5285-3602. E-mail: giselleabruzzese@gmail.com

Short title: Androgen excess and ovarian lipid metabolism

Keywords: Developmental programming, androgen excess, steroidogenesis, cholesterol, ovary.

Abstract

Prenatal androgen exposure affects reproductive functions and has been proposed as an underlying cause of polycystic ovary syndrome (PCOS). In this study, we aimed to investigate the impact of prenatal androgen exposure on ovarian lipid metabolism and to deepen our understanding of steroidogenesis regulation during adulthood. Pregnant rats were hyperandrogenized with testosterone and female offspring were studied when adult. This treatment leads to two different phenotypes: irregular ovulatory and anovulatory animals. Our results showed that prenatally hyperandrogenized (PH) animals displayed altered lipid and hormonal profile together with alterations in steroidogenesis and ovarian lipid metabolism. Moreover, PH animals showed alterations in the PPARg system, impaired mRNA levels of cholesterol receptors (*Ldl-r* and *Srb-1*) and decreased expression of the rate-limiting enzyme of de novo cholesterol production (*Hmgcr*). Anovulatory PH animals presented an increase of ovarian cholesteryl esters levels and lipid peroxidation index. Together with alterations in cholesterol metabolism, we found an impairment of the steroidogenic pathway in PH animals in a phenotype-specific manner. Regarding fatty acid metabolism, our results showed, in PH animals, an altered expression of *Srebp1* and *Atgl*, which are involved in fatty acid metabolism and triglycerides hydrolysis, respectively. In conclusion, fatty acid and cholesterol metabolism, which are key players in steroidogenesis acting as a source of energy and substrate for steroid production, were affected in animals exposed to androgens during gestation. These results suggest that prenatal androgen exposure leads to long-term effects that affect ovary lipid metabolism and ovarian steroid formation from the very first steps.

word count: 4972

Introduction

Prenatal exposure to androgens during fetal development impacts on several tissues and leads to reproductive and metabolic alterations during puberty and adulthood (Cardoso & Padmanabhan 2019). It has been widely shown, in several species, that prenatal androgen excess can program metabolic, endocrine and reproductive disturbances at postnatal life, and lead to the development of phenotypes that resemble the features of human Polycystic Ovary Syndrome (PCOS) (Padmanabhan & Veiga-Lopez 2013). The problems experienced by women with PCOS include ovarian infertility and reproductive abnormalities such as altered steroidogenesis (Sander et al. 2011) and impaired ovarian function (Franks *et al.* 2008).

It has been shown that the ovary is a target organ of fetal programming effects, particularly in cases of exposure to androgens during gestation (Puttabyatappa & Padmanabhan 2018). It is also known that fetal programming may have long-lasting effects on gene expression and physiological deregulations (Padmanabhan *et al.* 2016). However, the long-term impact of androgen excess during gestation on the ovary is still a matter of study.

The main functions of the ovaries are to produce oocytes and to secrete steroid hormones, thus regulating and supporting reproductive functions. All of these processes are mainly, but not exclusively, regulated by hormonal actions, including the action of gonadotropins and steroid hormones. In this regard, it has been suggested that lipids play a crucial role in reproductive functions (Kim *et al.* 2017; Dallel *et al.* 2018). Moreover, it is

known that alterations in the metabolic status, such as obesity and dyslipidemia, may have a negative impact on female fertility (Li & Ma 2018; Silvestris *et al.* 2018). It has been reported that lipid pathways are susceptible to being programmed in several tissues, including reproductive ones (Abruzzese *et al.* 2016; Calabuig-Navarro *et al.* 2017). However, whether prenatal androgen excess may affect ovarian functions and steroid production through lipid metabolism alterations requires further studies.

In the ovaries, lipids play a major role in reproductive and metabolic functions. Steroidogenesis, intracellular lipid metabolism, oxidative stress, among other processes, are controlled by the presence and activity of the Peroxisome proliferator-activated receptors (PPARs) nuclear receptors. It has been reported that the activation of PPARg (which includes its binding to PPARg co-activator 1 alpha, or PGC1a) modulates the synthesis of steroid hormones in granulosa cells. Furthermore, it has been shown that the disruption of this system has been reported to lead to female subfertility (Vélez *et al.* 2013).

During oogenesis and folliculogenesis, there is an accumulation of large amounts of sterols and triglycerides (TG). These are used as primary sources for ATP production or the synthesis of other lipid species (Dunning *et al.* 2014). Triglycerides are a major energy source and the predominant form of energy storage in several cell types, together with fatty acids, normally stored as lipid droplets in ovarian cells (Wu *et al.* 2010). Fatty acid and glucose oxidation provides energy substrates for oocyte development and steroidogenesis (Singh *et al.* 2013). As it is known that failures in energy metabolism may

lead to reproductive alterations (Dupont *et al.* 2018), ovarian lipids play a key role in ovarian energy balance.

Other lipids, such as phospholipids and sterols, have important functions as essential constituents of biological cell membranes, where they are crucial in membrane structural and physiological properties. Sterols are the main lipid species in the ovaries. They participate directly in the steroidogenic process, in which cholesterol acts as the limiting substratum in ovarian steroid synthesis (van Montfoort *et al.* 2014).

Moreover, regarding steroidogenesis, cholesterol availability is determinant for hormone synthesis. Steroidogenic cells of the ovary can obtain cholesterol from blood lipoproteins, suggested as the major sources, or by *de novo* synthesis. Steroids are involved in follicular development, ovulation, and pregnancy maintenance, and also participate in the regulation of gonadotropin secretion in the systemic circulation (Drummond 2006). Consequently, alterations in ovarian lipid metabolism may lead to infertility and several reproductive disorders, such as PCOS, among others (Lai *et al.* 2014). Taking all this evidence together, we aimed to investigate the effects of prenatal androgen exposure on ovarian lipid metabolism and steroidogenesis at adult age.

Material and methods

Animals and treatments

Virgin female rats of the Sprague Dawley strain were mated with fertile males of the same strain. Three females and one male were housed in each cage under controlled conditions

of light (12 h light, 12 h dark) and temperature (22 ºC). Animals were allowed free access to Purina rat chow (Cooperación SRL, Argentina) and water. Day 0 of pregnancy was estimated as the morning on which spermatozoa were observed in the vaginal fluid. As previously described (Abruzzese *et al.* 2016, 2019a), pregnant rats (N=10) received subcutaneous injections of 1 mg of free testosterone (T-1500; Sigma, St. Louis, MO, USA) dissolved in 100 µl corn oil from day 16 to day 19 of pregnancy. This hormonal paradigm mimics the fetal androgen surge that is observed in male rats when the reproductive axis in the fetus is established (Wolf 2002; Ramezani Tehrani *et al.* 2014). Another group (N=10) received only 100 µl of corn oil. Under the conditions of our animal facilities, spontaneous term labor occurs on day 22 of gestation. Female offspring were separated from males at 21 days of age. Those from hyperandrogenized mothers were the prenatally hyperandrogenized (PH) group and those from mothers injected with corn oil were the control group. Previous studies of our group have shown that, in this animal model, the treatment of the PH group leads to human PCOS like features, with impaired follicle count, ovarian cysts presence, biochemical hyperandrogenism and altered hormonal and metabolic profile (Abruzzese *et al.* 2016, 2019a).

Animals were euthanized by decapitation after anesthesia with carbon dioxide during adult age (three months of age). Ovaries were extracted, trunk blood was collected and serum was separated and kept at -80°C for further studies. All animals were randomly assigned for each assay considering their litter precedence. Care was taken when assigning and equilibrating the number of animals from each littermate to all the assays to prevent the maternal effect on the results.

All the procedures involving animals were conducted in accordance with the Animal Care and Use Committee of Consejo Nacional de Investigaciones Científicas y Técnicas (CONICET) 1996, Argentina. The present study was approved by the Ethics Committee of the School of Medicine of University of Buenos Aires.

Characterization of the estrous cyclicity

Estrous cycles were monitored daily by vaginal smears beginning at 70 days of age and until decapitation. As previously reported, the control group had regular cycles (4–6 days), whereas those animals prenatally exposed to androgens displayed mostly altered estrous cycles. Vaginal smears showed that 49.5% of the PH animals showed prolonged cycles lasting 7 days or more and were classified as irregular ovulatory animals (PHiov); and that 40.5% of the animals showed no cycles at all and were classified as anovulatory animals (PHanov) (Abruzzese *et al.* 2016; Heber *et al.* 2019). At three months of age, the entire PHanov group remained in diestrus; for that reason, and to allow comparison among groups, all animals were euthanized on the first diestrus after 90 days of age.

Serum determinations

Total cholesterol, high-density lipoprotein (HDL) and TG levels were quantified by colorimetric-enzymatic methods (Weiner Lab). The chromophoric product was measured at 505 nm for cholesterol, at 600 nm for HDL and at 490 nm for triglycerides. Low-density protein (LDL) cholesterol was estimated indirectly by the following formula: LDL = Total cholesterol - (HDL + Triglycerides/5) (Friedewald *et al.* 1972).

154 Luteinizing hormone (LH), follicle stimulating hormone (FSH), testosterone and
155 progesterone were quantified using radioimmunoassay (RIA), following the protocols
156 previously described (Lacau-Mengido *et al.* 1996; Abruzzese *et al.* 2019a). The intra- and
157 inter-assay coefficients were less than 10% and 13% for LH and FSH, respectively. The
158 utility range of testosterone assay was 25–1600 pg. The intra- and inter-assay variations
159 were 7.5 and 15.1%, respectively. Progesterone antiserum was highly specific for
160 progesterone and showed low cross-reactivity. The intra- and inter-assay coefficients of
161 variation were 10.9 and 12.8%, respectively. Serum estradiol levels were quantified with
162 Cobase immunoassay analyzers using an Electro Chemiluminescence Immuno Assay
163 (ECLIA) following the manufacturer's instructions. The intra- and inter-assay coefficients of
164 variation were 13.2 and 7.08%.
165
166 **Ovarian lipid content**
167 Lipid content was analyzed by thin layer chromatography (TLC). Both ovaries per animal
168 were homogenized in 1 ml phosphate-buffered saline (PBS) and protein content in the
169 homogenates was measured by the Bradford assay. Tissue lipids were extracted from 500
170 µl of each homogenate by two rounds of organic extraction in methanol: chloroform (2:1),
171 following the method of Bligh & Dyer (1959). The lipids extracted were developed by thin
172 layer chromatography in 0.2 mm silica gel plates (Merck, Darmstadt, Germany), using
173 hexane: ethyl ether: acetic acid (80:20:2, v:v:v) as the developing solvent mixture, as
174 previously reported (Kurtz *et al.* 2010). Samples were developed with known amounts of
175 lipid standards on the same plate. Lipid species were stained with iodine vapors and the

plate was scanned for further identification and quantification of the lipid species by comparison with known amounts of standards. Densitometric analysis of the area intensity of each spot was performed with the ImageJ software. The lipid content was expressed as ug lipids/mg protein.

Gene expression analysis

In order to assess lipid metabolism, the expression of *Pparg* and *Pgc1* was analyzed. Fatty acid metabolism and availability from triglycerides was evaluated by measuring mRNA levels of *Srebp1* and *Atgl*, respectively. To evaluate cholesterol bioavailability, the mRNA expression of the cholesterol receptors: *Ldl-r* and *Srb1* was assessed, and *de novo* cholesterol synthesis was assessed, by measuring the mRNA expression of its limiting enzyme, 3-hydroxy-3-methylglutaryl-CoA reductase (*Hmgcr*).

All mRNA levels were quantified by Real-Time PCR analysis. Briefly, total mRNA from ovarian tissue was extracted using RNAzol RT (MRC gene, Molecular Research Center, Cincinnati, OH, USA), following the manufacturer's instructions. For each sample, cDNA was synthesized from 1 µg mRNA using random primer hexamers (Invitrogen-Life Technologies, Buenos Aires, Argentina). Real-time PCR analysis was performed from this cDNA (2.5 µL) in 10 µL reaction buffer containing a 20 mM dNTPs mix, GoTaq Polymerase (Promega), Eva Green 20x (Biotium Hayward, CA, USA) and gene-specific primers in a total volume of 12.5 µL. The qPCR conditions started with a denaturation step at 95ºC for 5 min and followed by up to 40 cycles of denaturation (95ºC), annealing (see temperature for each primer in table 1) and primer extension (72ºC). The amplified products were

198 quantified by fluorescence, using the Rotor Gene 6000 Corbett, and mRNA abundance was
199 normalized to the amount of 60s Ribosomal protein L32 (L32) and Proteasome Subunit
200 Beta 2 (Psmb2) considering the geometric media. Both L32 and Psmb2 were validated as
201 reference genes as the variance between treatments did not differ. In order to check for
202 DNA contamination, for L32, a control without reverse transcription was included to
203 ensure that amplification was only from mRNA. All of the amplicons for the different
204 genes were characterized according to their melting temperature and size. Each qPCR run
205 included a no-template control. The reaction conditions and quantities of cDNA added
206 were calibrated such that the assay response was linear with respect to the amount of
207 input cDNA for each pair of primers. Gene expression was quantified using the $2^{-\Delta\Delta Ct}$
208 method (Livak & Schmittgen 2001). Results are expressed as a fold value of the controls.
209 The primers are shown in Table 1.
210
211 **Protein expression analysis**
212 Protein expression in ovarian tissue was determined by Western blot analysis. Briefly,
213 ovarian tissue was lysed for 20 min at 4 ºC in lysis buffer (20 mM Tris-HCl, pH= 8.0, 137
214 mM NaCl, 1% Nonidet P-40 and 10% glycerol) supplemented with protease inhibitors
215 (Sigma-Aldrich, St. Louis, MO, USA). The lysate was centrifuged at 4 ºC for 10 min at
216 10,000 g and the pellet discarded. Protein concentrations in the supernatant were
217 measured by the Bradford assay (Bio-Rad, Hercules, CA, USA). After boiling for 5 min, 30
218 µg of each protein was applied to a 12% SDS-polyacrylamide gel and electrophoresis was
219 performed at 80 Volts for 1.5 h. The separated proteins were transferred onto

nitrocellulose membranes in transfer buffer (20% methanol, vol/vol; 0.19 M glycine; 0.025 M Tris-Base, pH= 8.3) for 1 h at 400 mA and 4 ºC. Blocking was carried out for 1 h at room temperature in 5% non-fat milk in PBS and membranes were incubated with the primary antibody (Table 2), diluted in 1% bovine serum albumin in PBS, overnight at 4 ºC. The protein bands were visualized by incubating the blots with horseradish peroxidase-conjugated secondary antibody Goat anti-rabbit IgG IgG H&L, HRP (1:1500, #1706515, BioRad) or anti-mouse IgG HRP (1:5000, ab6728, Abcam) for 1 h, followed by ECL Western Blotting Substrate (Thermo Scientific, IL, USA). Rainbow-colored protein mass markers (14.3-200 kDa, Bio-Rad) were applied to samples as molecular weight standards.

The consistency of protein loading was evaluated by staining the membranes with Ponceau-S. The expression of the target proteins was normalized for total protein staining to adjust for unequal loading. The images were captured in a chemiluminescence imaging system (GeneGnomeXRQ, Syngene), and the intensities (area x density) of the individual bands were evaluated with ImageJ software. When quantified, the intensity of each protein band was normalized to the total protein in individual samples to adjust for unequal loading and transfer (Roberti *et al.* 2018).

Co-Immunoprecipitation (co-IP) of PPARg and PGC1a

To evaluate PPARg interaction with its co-activator PGC1a, a co-immunoprecipitation was performed. Ovarian tissue (25 mg for each sample) was homogenized in 500ul of non-denaturing lysis buffer (200mM Tris-HCl pH=8, 137 mM NaCl, 10% glycerol, % NP-40, 2nM EDTA pH=8) supplemented with protease inhibitors (Sigma, USA). Lysate was incubated in

agitation during 2hs at 4°C. After a centrifugation at 10000g, supernatant was recovered and 1 ug of anti PPARg1+2 (ab41928,Abcam, UK) was added to the samples, and incubated overnight in agitation at 4°C. Antibody complexes were precipitated using Protein G Plus Agarose (Santa Cruz) overnight at 4°C. Complexes were pelleted and washed 3 times in modified RIPA buffer (50 mM Tris-HCl pH=8, 150 mM NaCl, 2 mM EDTA pH=8, 1% NP-40, 0,5% sodium deoxycholate, 0,2% SDS) containing protease inhibitors to eliminate non-specific interactions. After the last wash, all the samples were resuspended in 50 ul of 2X Laemli buffer (4% SDS, 20% glycerol, 0,004% bromophenol blue, 0,125M Tris-Cl pH= 6,8, 10% 2-mercaptoethanol) which was added to the precipitated containing the beads and bound protein complexes and the beads were denatured by boiling at 95°C for 7 minutes. Samples were analyzed by Western blot to identify the coprecipitating effector protein using PGC1a antibody (sc13067, Santa Cruz Biotechnology, USA), as described above.

Lipid peroxidation

The amount of malondialdehyde (MDA) formed from the breakdown of polyunsaturated fatty acids was taken as an index of peroxidation reaction. The method quantifies MDA as the product of lipid peroxidation that reacts with trichloracetic acid–thiobarbituric acid–HCl (15% (w/v), 0.375% (w/v) and 0.25 M, respectively) yielding a red compound that absorbs at 535nm (Motta *et al.* 2001). Homogenates of ovarian tissue were treated with trichloroacetic acid–thiobarbituric acid–HCl and heated for 15 min in boiling water bath. After cooling, the flocculent precipitate was removed by centrifugation at 1000 g for 10

min. The absorbance of samples was determined at 535 nm. Content of thiobarbituric acid reactants were expressed as nmol MDA formed/g tissue.

Statistical analysis

Data was analyzed by ANOVA with *post hoc* Tukey test. Data normality was checked using the Shapiro-Wilks test. The equality of variance was tested using the Levene test. If required, Log10 transformation was used to normalize the distribution of data and to the statistical analysis. Data were back-transformed for presentation. Statistical significance was considered as $p<0.05$. The sample size for the experimental procedures was calculated using G*power 3 (Faul *et al.* 2007). Statistical analyses were carried out using the Instat program (GraphPad Software, San Diego, CA, USA).

Results

Hormonal and metabolic determinations

Prenatal androgenization did not affect the body weight at three months of age, while ovarian weight was decreased in the PHanov phenotype (Table 3). Similar to our previous findings (Abruzzese *et al.* 2019b), lipid profile was altered at adulthood in PH animals, which showed increased levels of LDL-cholesterol ($p<0.01$) and TG ($p<0.01$) as compared with the control group. Regarding hormonal steroid profile, as previously found (Heber *et al.* 2019), prenatal androgenization led to an increase in testosterone levels in the PHanov group ($p<0.01$) and a decrease in estradiol levels in both PHiov and PHanov groups ($p<0.05$), without alterations in progesterone levels ($p>0.05$). Moreover, neither of the PH

286 groups showed altered levels of the gonadotropins FSH and LH as compared to the control
287 group ($p>0.05$).
288
289 **Ovary lipid content**
290 We found no changes in ovarian TG, fatty acids and phospholipids ovary content in the PH
291 group as compared to the control group (Fig.1A, B and C, respectively, $p>0.05$). Regarding
292 cholesterol content, we found no differences in the PH group as compared to control
293 group (Fig.1D, $p<0.05$), but found higher levels of cholesteryl esters in the PHanov
294 phenotype as compared to the PHiov and control groups (Fig.1E, $p<0.05$).
295
296 **Ovarian lipid metabolism**
297 Prenatal androgenization affected PPARg and its coactivator (PGC1a) expression and
298 interaction. We found a decrease in PPARg mRNA (Fig. 2A, $p<0.01$) and protein levels (Fig.
299 2B, $p<0.05$) in the PH phenotypes as compared to the control group. Moreover, PGC1a
300 mRNA and protein levels (Fig. 2C and D, $p<0.05$) were decreased in the PHiov phenotype.
301 Co-immunoprecipitation results showed a decreased interaction between PPARg and
302 PGC1a in the PH phenotypes as compared to controls (Fig. 2E, $p<0.05$).
303 Fatty acid metabolism was also impaired by prenatal androgen exposure. We found that
304 the mRNA levels of the master regulator of fatty acid metabolism *Srebp1* were decreased
305 in both PH phenotypes as compared to the control group (Fig. 3A, $p<0.01$). Moreover, we
306 found that the mRNA levels of *Atgl*, a key enzyme involved in the initial step of

intracellular hydrolysis of TG, were increased in both PH phenotypes, with the highest levels in the PHiov phenotype (Fig. 3B, $p<0.01$).

We also found that prenatal androgenization altered ovarian cholesterol pathway. Our results showed that the cholesterol receptors, LDL-R and SRB1, were altered in the PH groups. In the case of the PHanov phenotype, the mRNA levels of Ldl-r were increased (Fig. 4A, $p<0.01$), while in the PHiov phenotype, the mRNA levels of Srb1 were decreased (Fig. 4B, $p<0.05$). Moreover, the mRNA levels of *Hmgcr,* a key enzyme in cholesterol *de novo* synthesis, were lower in the PH group than in the control group (Fig 4C, $p<0.01$).

Ovarian lipid peroxidation

The lipid peroxidation index was evaluated by the content of ovarian MDA. We found that lipid peroxidation index was increased in the PHanov phenotype as compared to the control group (Fig. 5, $p<0.05$).

Ovarian steroidogenesis

Ovarian steroidogenic pathway was evaluated to study the relation between steroidogenesis and lipid metabolism (Fig 6). The protein levels of StAR were increased in the PHanov phenotype ($p<0.05$). The protein levels of 3BHSD and CYP17, limiting enzymes in progesterone and androgen synthesis, respectively, remained unaltered in the PH phenotypes ($p>0.05$). The protein levels of 17BHSD, involved in testosterone synthesis, were decreased in the PHanov phenotype and showed a tendency to decrease in the PHiov phenotype ($p<0.05$). The protein levels of CYP19 (aromatase), involved in estradiol

329 synthesis, were increased in the PHiov phenotype and showed a tendency to increase in
330 the PHanov phenotype ($p<0.05$).

331 **Discussion**

332 Reproductive functions depend on hormonal regulation and also on energy storage and
333 availability. Lipids play important roles in ovarian functions, acting as sources of energy,
334 and as substrates for several intracellular processes (Dallel *et al.* 2018).
335 Prenatal exposure to a suboptimal intrauterine environment could lead to long term
336 effects affecting reproductive functions. To study the impact of fetal programming of
337 animals exposed to androgens, we reproduced a rodent model of prenatal androgen
338 excess widely used (Wolf 2002; Ramezani Tehrani *et al.* 2014; Abruzzese *et al.* 2016,
339 2019a, b; Heber *et al.* 2019). Here, using this model, we addressed the question of
340 whether ovarian lipid metabolism and specifically cholesterol metabolism are impaired in
341 these animals when adults.
342 Prenatal androgen exposure may negatively impact on gonadal development, conditioning
343 its growth and functions in postnatal life. In this regard, we found a decreased ovarian
344 weight in the PHanov phenotype, which could account, at least in part, for the more
345 severe ovarian defects found in this phenotype.
346 In this animal model, the lipid profile was found altered together with an imbalance in
347 steroid hormone profile, thus highlighting the effect of steroid hormones on lipid
348 metabolism (Kakuta *et al.* 2013; Meng *et al.* 2015). We found no changes in gonadotropins
349 levels, as we have previously reported at pubertal age (Abruzzese *et al.* 2019a). However,
350 although gonadotropins levels may remain unaltered, defects in their pulsatility are

possible (Yan *et al.* 2014). Moreover, it is important to highlight that, together with gonadotropins, lipids and insulin are also involved in ovarian steroid production. In this regard, we have previously shown that PH animals show insulin resistance and impaired ovarian insulin signaling (Heber *et al.* 2019); and here, we report that ovarian lipid pathways are also affected. Taking together, these data highlight the role of energetic ovarian defects, as those given by alterations on lipids and insulin pathways, as contributing factors to altered steroid production in hyperandrogenic contexts.

The master regulator of lipid metabolism PPARg is also involved in female reproductive functions, and particularly it has been reported that PPARg regulates steroidogenic enzymes (Vélez *et al.* 2013). Alterations in PPARg system have already been reported in PCOS patients and animal models (Chen *et al.* 2015a; Cao *et al.* 2019). Here, we found that the expression of PPARg and its co-activator, PCG-1a, are decreased in PH animals. Moreover, we found that PPARg activation was decreased in these animals. These results extend our previous findings about the role of PPARg system in androgenic contexts (Abruzzese *et al.* 2019a). This evidence shows that this system's expression pattern could change across different life stages in PH animals during post-natal life (Abruzzese *et al.* 2019a), as it has already been suggested in sheep (Ortega *et al.* 2010). In accordance with our results, it has been shown that PCOS adult women show a downregulation of PPARg expression in ovarian granulosa cells (Cao *et al.* 2019), and that the treatment with thiazolidinediones (high-affinity ligands for PPARg that lead to its activation) has positive effects on reproductive function and ovulation rate in these patients (Froment & Touraine

2006). These results suggest that, in androgenic contexts, PPARg system activation may be impaired and highlights the crucial role of this system in ovarian functions.

During oogenesis, maturing oocytes accumulate neutral lipids that are essential for both energy production and synthesis of other lipid molecules. For example, fatty acids are used as an energy source during oocyte maturation. Here, we showed that although fatty acid content was not altered in the ovaries of the PH group, fatty acid metabolism was impaired. Gene expression of *Srebp1*, which regulates several genes involved in fatty acid synthesis, was decreased in PH animals. On the other hand, mRNA expression of *Atgl*, which participates in the initial steps in triglycerides hydrolysis, was increased in the PH group. Taken together, these results suggest that although prenatal androgenization affected fatty acid synthesis, there is compensation between two different pathways for obtaining fatty acids.

Oxidative stress is associated with decreased female fertility. In particular, fatty acid peroxidation has been suggested as one of the main sources that can affect gamete viability, negatively impacting fertility (Agarwal *et al.* 2012). Ovarian oxidative stress plays a crucial role in PCOS, ovarian senescence and age-related decline of reproductive function (Yildirim *et al.* 2007; Aiken *et al.* 2013). Moreover, it has been shown that testosterone has pro-oxidant properties and is able to induce oxidative stress in different mammalian tissues, as for example, in female placenta (Zhu *et al.* 1997; Alonso-Alvarez *et al.* 2007). In this study, we found that the anovulatory phenotype showed increased levels of lipid peroxidation. This result shows that increased testosterone exposure during development and postnatal life could lead to an increased lipid peroxidation, contributing

394 to the reproductive alterations and infertility already reported in this phenotype (Ferreira
395 *et al.* 2019).
396 Cholesterol is essential for ovarian steroidogenesis (Strauss 2019). Ovarian tissue may
397 synthesize *de novo* cholesterol being HMGCR a limiting enzyme in this process. The role of
398 HMGCR in PCOS pathology has been highlighted in other studies. In this regard, in a
399 murine model of PCOS, it was shown a repression in the transcription of HMGCR, and
400 other genes involved in lipid metabolism (Salilew-Wondim *et al.* 2015). Moreover, in PCOS
401 patients, it has been described that *Hmgcr* may act as a modifier gene in PCOS (Xu *et al.*
402 2010). Together with these findings, it has been shown that HMGCR expression, at least in
403 hepatic cells, can be induced by estrogenic action, as the *Hmgcr* promoter has estrogen
404 response elements (Meng *et al.* 2015). Therefore, low levels of estradiol in the PH animals
405 could account for the decreased expression of *Hmgcr* that we found.
406 Despite the possibility of *de novo* cholesterol synthesis, as there is a high demand in
407 cholesterol bioavailability in steroidogenic cells, it may also be captured from plasma
408 involving two different receptors: LDL-R and SR-B1 (Wang & Menon 2005; Lai *et al.* 2014).
409 In rodents, it has been reported that both receptors are important in cholesterol
410 trafficking and steroid biosynthesis (Chang *et al.* 2017). It has been shown that female
411 mice knockout for *Sr-b1* or *Ldl-r* are infertile (Miettinen *et al.* 2001) or show alterations in
412 the estrous cycle, steroidogenesis and folliculogenesis (Guo *et al.* 2015). In accordance
413 with these data, our results showed that the PH animals presented an altered expression
414 of ovarian cholesterol receptors. These results indicate that in both PH phenotypes,
415 ovarian cholesterol trafficking pathway is altered. In the case of PHanov animals, the

entering of cholesterol to the cell would be promoted in the PHanov phenotype due to the increase in *Ldl-r* mRNA levels. While in the PHiov phenotype, cholesterol entrance is also altered, showing a decrease in *Sr-b1* mRNA levels, but no alterations in *Ldl-r* expression, suggesting that LDL cholesterol may be used as a preferential source for steroidogenesis. It has been reported that knock-out *Srb1* female mice are infertile but do not exhibit estrous cycle defects or altered number of ovulated oocytes (Trigatti *et al.* 1999). Moreover, testosterone (Langer *et al.* 2002) and estradiol (Lopez *et al.* 2002) can up-regulate *Srb1* expression, and it was shown that some mutations of *Srb1* that affect this gene expression, decreasing it, are associated with low estradiol levels (Strauss 2019). In agreement with these reports, our PHiov animals showed low expression of *Srb1* and also low levels of estradiol. However, as we have shown in a previous report, these animals are able to become pregnant but with a lower efficacy than control females, showing some degree of subfertility (Ferreira *et al.* 2019). The different expression of S*rb1* between PHanov and PHiov animals may be due to the testosterone and estradiol levels, while both PH groups showed low estradiol levels, PHanov animals showed high testosterone, which could be acting up-regulating *Srb1* expression and therefore contributing to high cholesterol trafficking in the ovaries of these animals.

The quantity of sterol ester stored depends on the availability of cholesterol and the cell's steroidogenic activity. In steroidogenic cells such as ovary and testis, the formation of lipid droplets is hormonally regulated (Hu *et al.* 2010); therefore, alterations in hormone production or levels could affect cholesterol esterification and lipid droplets depot (Strauss 2019). In our animal model, we found that PH animals had altered hormonal

438 balance together with impaired ovarian steroid production. Particularly, in the PHanov
439 phenotype, we found an increase in cholesterol esters. This increase in cholesterol
440 esterification in this phenotype is probably related to the increased intake of cholesterol
441 through *Ldl-r* and testosterone synthesis.
442 All of these derangements in the cholesterol pathway and the PPARg system also affected
443 steroidogenesis. When we analyzed steroidogenic mediators, we found alterations in
444 several of them in a phenotype-specific manner. In the PHiov phenotype, little alterations
445 were found regarding steroidogenesis. However, the fact that the protein expression of
446 17BHSD tended to decrease is consistent with the lack of increased testosterone levels.
447 This phenotype also showed low estradiol levels despite increased CYP19 (aromatase)
448 protein expression. This could be due to defects in aromatase activity, which have been
449 previously reported in PCOS women (Chen *et al.* 2015b). Taking all of these together, the
450 decreased estradiol levels could contribute to an altered hormonal balance that may
451 influence reproductive functions in this phenotype.
452 In the PHanov phenotype, we found alterations in StAR, 17BHSD and CYP19 protein
453 expression. This phenotype exhibited a favoring to high steroid synthesis, as shown by
454 increased StAR protein expression, consistent with the increased testosterone levels
455 found. However, unexpectedly, we found a decreased protein expression of 17BHSD. A
456 possibility is that although enzyme expression is down, its activity may be increased.
457 Similar to our findings, other authors have also reported this paradoxical result regarding
458 the decreased expression of enzymes involved in androgen synthesis and increased
459 androgen production (Ortega *et al.* 2013; Padmanabhan *et al.* 2014).

460 It is important to highlight that although the steroidogenic factors and enzymes were also
461 altered at early stages of life (Abruzzese *et al.* 2019a), here, we found that at adulthood,
462 the pattern is changed as compared with that observed at 60 days of age. These results
463 suggest that the long term effects of developmental programming by androgen excess
464 may change through life. These data are consistent with a report from Padmanabhan et al.
465 (2014) in prenatally androgenized sheep, who also found that steroidogenic mediators are
466 altered and change in an age-specific manner (Padmanabhan *et al.* 2014).
467 In conclusion, our results show that prenatal androgen excess exerts long-term effects on
468 ovarian functions affecting ovarian lipid metabolism and particularly affecting the
469 steroidogenic pathway from the very first steps involving cholesterol availability and
470 synthesis.
471

472 **Declaration of interest**

473 Authors have nothing to declare.

474 **Acknowledgements**

475 We thank Enzo Cuba and Marcela Marquez for their technical support in the animal care.
476

477 **Funding**

478 This study was supported by grants from Agencia Nacional de Promoción Científica y
479 Tecnológica (ANPCyT) (Grant PICT 632/2016) and Fundación Roemmers, Argentina. GAA,
480 is supported by a fellowship awarded by CONICET, MJF is supported by a fellowship of
481 ANPCyT. ABM is a PhD principal investigator from CONICET.

References

Abruzzese GA, Heber MF, Ferreira SR, Velez LM, Reynoso R, Pignataro OP & Motta AB 2016 Prenatal hyperandrogenism induces alterations that affect liver lipid metabolism. *Journal of Endocrinology* **230** 67–79. (doi:10.1530/JOE-15-0471)

Abruzzese GA, Heber MF, Campo Verde Arbocco F, Ferreira SR & Motta AB 2019a Fetal programming by androgen excess in rats affects ovarian fuel sensors and steroidogenesis. *Journal of Developmental Origins of Health and Disease* 1–14. (doi:10.1017/S2040174419000126)

Abruzzese GA, Heber MF, Ferrer MJ, Ferreira SR, Silva AF & Motta AB 2019b Effects of in utero androgen excess and metformin treatment on hepatic functions. *Molecular and Cellular Endocrinology*. (doi:10.1016/j.mce.2019.03.006)

Agarwal A, Aponte-Mellado A, Premkumar BJ, Shaman A & Gupta S 2012 The effects of oxidative stress on female reproduction: a review. *Reproductive Biology and Endocrinology: RB&E* **10** 49. (doi:10.1186/1477-7827-10-49)

Aiken CE, Tarry-Adkins JL & Ozanne SE 2013 Suboptimal nutrition in utero causes DNA damage and accelerated aging of the female reproductive tract. *The FASEB Journal* **27** 3959–3965. (doi:10.1096/fj.13-234484)

Alonso-Alvarez C, Bertrand S, Faivre B, Chastel O & Sorci G 2007 Testosterone and oxidative stress: the oxidation handicap hypothesis. *Proceedings of the Royal Society B: Biological Sciences* **274** 819–825. (doi:10.1098/rspb.2006.3764)

Bligh EG & Dyer WJ 1959 A rapid method of total lipid extraction and purification. *Canadian Journal of Biochemistry and Physiology* **37** 911–917. (doi:10.1139/o59-099)

Calabuig-Navarro V, Haghiac M, Minium J, Glazebrook P, Ranasinghe GC, Hoppel C, Hauguel de-Mouzon S, Catalano P & O'Tierney-Ginn P 2017 Effect of Maternal Obesity on Placental Lipid Metabolism. *Endocrinology* **158** 2543–2555. (doi:10.1210/en.2017-00152)

Cao J, Maowulieti G & Yu T 2019 Effect of testosterone on the expression of PPARγ mRNA in PCOS patients. *Experimental and Therapeutic Medicine* **17** 1761–1765. (doi:10.3892/etm.2018.7101)

Cardoso RC & Padmanabhan V 2019 Prenatal Steroids and Metabolic Dysfunction: Lessons from Sheep. *Annual Review of Animal Biosciences* **7** 337–360. (doi:10.1146/annurev-animal-020518-115154)

515 Chang X-L, Liu L, Wang N, Chen Z-J & Zhang C 2017 The function of high-density
516 lipoprotein and low-density lipoprotein in the maintenance of mouse ovarian
517 steroid balance. *Biology of Reproduction* **97** 862–872. (doi:10.1093/biolre/iox134)

518 Chen M-J, Chou C-H, Chen S-U, Yang W-S, Yang Y-S & Ho H-N 2015a The effect of
519 androgens on ovarian follicle maturation: Dihydrotestosterone suppress FSH-
520 stimulated granulosa cell proliferation by upregulating PPARγ-dependent PTEN
521 expression. *Scientific Reports* **5** 18319. (doi:10.1038/srep18319)

522 Chen J, Shen S, Tan Y, Xia D, Xia Y, Cao Y, Wang W, Wu X, Wang H, Yi L *et al.* 2015b The
523 correlation of aromatase activity and obesity in women with or without polycystic
524 ovary syndrome. *Journal of Ovarian Research* **8** 11. (doi:10.1186/s13048-015-0139-
525 1)

526 Dallel S, Tauveron I, Brugnon F, Baron S, Lobaccaro JMA & Maqdasy S 2018 Liver X
527 Receptors: A Possible Link between Lipid Disorders and Female Infertility.
528 *International Journal of Molecular Sciences* **19**. (doi:10.3390/ijms19082177)

529 Drummond AE 2006 The role of steroids in follicular growth. *Reproductive Biology and*
530 *Endocrinology* **4** 16. (doi:10.1186/1477-7827-4-16)

531 Dunning KR, Russell DL & Robker RL 2014 Lipids and oocyte developmental competence:
532 the role of fatty acids and β-oxidation. *Reproduction* **148** R15–R27.
533 (doi:10.1530/REP-13-0251)

534 Dupont J, Bertoldo MJ & Rak A 2018 Energy Sensors in Female and Male Reproduction and
535 Fertility. *International Journal of Endocrinology* **2018**. (doi:10.1155/2018/8285793)

536 Faul F, Erdfelder E, Lang A-G & Buchner A 2007 G*Power 3: a flexible statistical power
537 analysis program for the social, behavioral, and biomedical sciences. *Behavior*
538 *Research Methods* **39** 175–191. (doi:10.3758/bf03193146)

539 Ferreira SR, Goyeneche AA, Heber MF, Abruzzese GA, Telleria CM & Motta AB 2019
540 Prenatally androgenized female rats develop uterine hyperplasia when adult.
541 *Molecular and Cellular Endocrinology* **499** 110610.
542 (doi:10.1016/j.mce.2019.110610)

543 Franks S, Stark J & Hardy K 2008 Follicle dynamics and anovulation in polycystic ovary
544 syndrome. *Human Reproduction Update* **14** 367–378.
545 (doi:10.1093/humupd/dmn015)

546 Friedewald WT, Levy RI & Fredrickson DS 1972 Estimation of the Concentration of Low-
547 Density Lipoprotein Cholesterol in Plasma, Without Use of the Preparative
548 Ultracentrifuge. *Clinical Chemistry* **18** 499–502.

549 Froment P & Touraine P 2006 Thiazolidinediones and Fertility in Polycystic Ovary
550 Syndrome (PCOS). *PPAR Research* **2006**. (doi:10.1155/PPAR/2006/73986)

551 Guo T, Zhang L, Cheng D, Liu T, An L, Li W-P & Zhang C 2015 Low-density lipoprotein
552 receptor affects the fertility of female mice. *Reproduction, Fertility, and*
553 *Development* **27** 1222–1232. (doi:10.1071/RD13436)

554 Heber MF, Ferreira SR, Abruzzese GA, Raices T, Pignataro OP, Vega M & Motta AB 2019
555 Metformin improves ovarian insulin signaling alterations caused by fetal
556 programming. *Journal of Endocrinology* **1**. (doi:10.1530/JOE-18-0520)

557 Hu J, Zhang Z, Shen W-J & Azhar S 2010 Cellular cholesterol delivery, intracellular
558 processing and utilization for biosynthesis of steroid hormones. *Nutrition &*
559 *Metabolism* **7** 47. (doi:10.1186/1743-7075-7-47)

560 Kakuta H, Matsushita A, Arikawa K, Iguchi T & Sato T 2013 Cholesterol homeostasis in the
561 ovaries of neonatally diethylstilbestrol-treated mice. *Experimental and Clinical*
562 *Endocrinology & Diabetes: Official Journal, German Society of Endocrinology [and]*
563 *German Diabetes Association* **121** 94–101. (doi:10.1055/s-0033-1333780)

564 Kim N, Nakamura H, Masaki H, Kumasawa K, Hirano K & Kimura T 2017 Effect of lipid
565 metabolism on male fertility. *Biochemical and Biophysical Research*
566 *Communications* **485** 686–692. (doi:10.1016/j.bbrc.2017.02.103)

567 Kurtz M, Capobianco E, Martínez N, Fernández J, Higa R, White V & Jawerbaum A 2010
568 Carbaprostacyclin, a PPARdelta agonist, ameliorates excess lipid accumulation in
569 diabetic rat placentas. *Life Sciences* **86** 781–790. (doi:10.1016/j.lfs.2010.03.008)

570 Lacau-Mengido IM, Libertun C & Becú-Villalobos D 1996 Different Serotonin Receptor
571 Types Participate in 5-Hydroxytryptophan-Induced Gonadotropins and Prolactin
572 Release in the Female Infantile Rat. *Neuroendocrinology* **63** 415–421.
573 (doi:10.1159/000127089)

574 Lai H, Jia X, Yu Q, Zhang C, Qiao J, Guan Y & Kang J 2014 High-fat diet induces significant
575 metabolic disorders in a mouse model of polycystic ovary syndrome. *Biology of*
576 *Reproduction* **91** 127. (doi:10.1095/biolreprod.114.120063)

577 Langer C, Gansz B, Goepfert C, Engel T, Uehara Y, von Dehn G, Jansen H, Assmann G & von
578 Eckardstein A 2002 Testosterone up-regulates scavenger receptor BI and
579 stimulates cholesterol efflux from macrophages. *Biochemical and Biophysical*
580 *Research Communications* **296** 1051–1057. (doi:10.1016/s0006-291x(02)02038-7)

581 Li X & Ma X 2018 Effects of dyslipidemia on in-vitro fertilization/intracytoplasmic sperm
582 injection (IVF/ICSI) pregnancy outcome in patients with polycystic ovary
583 syndrome(PCOS). *Fertility and Sterility* **110** e198.
584 (doi:10.1016/j.fertnstert.2018.07.576)

585 Livak KJ & Schmittgen TD 2001 Analysis of Relative Gene Expression Data Using Real-Time
586 Quantitative PCR and the 2−ΔΔCT Method. *Methods* **25** 402–408.
587 (doi:10.1006/meth.2001.1262)

588 Lopez D, Sanchez MD, Shea-Eaton W & McLean MP 2002 Estrogen Activates the High-
589 Density Lipoprotein Receptor Gene via Binding to Estrogen Response Elements and
590 Interaction with Sterol Regulatory Element Binding Protein-1A. *Endocrinology* **143**
591 2155–2168. (doi:10.1210/endo.143.6.8855)

592 Meng Y, Lv P-P, Ding G-L, Yu T-T, Liu Y, Shen Y, Hu X-L, Lin X-H, Tian S, Lv M *et al.* 2015 High
593 Maternal Serum Estradiol Levels Induce Dyslipidemia in Human Newborns via a
594 Hepatic HMGCR Estrogen Response Element. *Scientific Reports* **5** 10086.
595 (doi:10.1038/srep10086)

596 Miettinen HE, Rayburn H & Krieger M 2001 Abnormal lipoprotein metabolism and
597 reversible female infertility in HDL receptor (SR-BI)–deficient mice. *Journal of*
598 *Clinical Investigation* **108** 1717–1722.

599 van Montfoort APA, Plösch T, Hoek A & Tietge UJF 2014 Impact of maternal cholesterol
600 metabolism on ovarian follicle development and fertility. *Journal of Reproductive*
601 *Immunology* **104–105** 32–36. (doi:10.1016/j.jri.2014.04.003)

602 Motta AB, Estevez A, Franchi A, Perez-Martinez S, Farina M, Ribeiro ML, Lasserre A &
603 Gimeno MF 2001 Regulation of lipid peroxidation by nitric oxide and PGF2alpha
604 during luteal regression in rats. *Reproduction (Cambridge, England)* **121** 631–637.
605 (doi:10.1530/rep.0.1210631)

606 Ortega HH, Rey F, Velazquez MML & Padmanabhan V 2010 Developmental Programming:
607 Effect of Prenatal Steroid Excess on Intraovarian Components of Insulin Signaling
608 Pathway and Related Proteins in Sheep. *Biology of Reproduction* **82** 1065–1075.
609 (doi:10.1095/biolreprod.109.082719)

610 Ortega I, Sokalska A, Villanueva JA, Cress AB, Wong DH, Stener-Victorin E, Stanley SD &
611 Duleba AJ 2013 Letrozole increases ovarian growth and Cyp17a1 gene expression
612 in the rat ovary. *Fertility and Sterility* **99** 889–896.
613 (doi:10.1016/j.fertnstert.2012.11.006)

614 Padmanabhan V & Veiga-Lopez A 2013 Animal models of the polycystic ovary syndrome
615 phenotype. *Steroids* **78** 734–740. (doi:10.1016/j.steroids.2013.05.004)

616 Padmanabhan V, Salvetti NR, Matiller V & Ortega HH 2014 Developmental programming:
617 prenatal steroid excess disrupts key members of intraovarian steroidogenic
618 pathway in sheep. *Endocrinology* **155** 3649–3660. (doi:10.1210/en.2014-1266)

619 Padmanabhan V, Cardoso RC & Puttabyatappa M 2016 Developmental Programming, a
620 Pathway to Disease. *Endocrinology* **157** 1328–1340. (doi:10.1210/en.2016-1003)

621 Puttabyatappa M & Padmanabhan V 2018 Developmental Programming of Ovarian
622 Functions and Dysfunctions. In *Vitamins and Hormones*, pp 377–422. Elsevier.
623 (doi:10.1016/bs.vh.2018.01.017)

624 Ramezani Tehrani F, Noroozzadeh M, Zahediasl S, Piryaei A, Hashemi S & Azizi F 2014 The
625 Time of Prenatal Androgen Exposure Affects Development of Polycystic Ovary
626 Syndrome-Like Phenotype in Adulthood in Female Rats. *International Journal of*
627 *Endocrinology and Metabolism* **12**. (doi:10.5812/ijem.16502)

628 Roberti SL, Higa R, White V, Powell TL, Jansson T & Jawerbaum A 2018 Critical role of
629 mTOR, PPARγ and PPARδ signaling in regulating early pregnancy decidual function,
630 embryo viability and feto-placental growth. *Molecular Human Reproduction* **24**
631 327–340. (doi:10.1093/molehr/gay013)

632 Salilew-Wondim D, Wang Q, Tesfaye D, Schellander K, Hoelker M, Hossain MM & Tsang BK
633 2015 Polycystic ovarian syndrome is accompanied by repression of gene signatures
634 associated with biosynthesis and metabolism of steroids, cholesterol and lipids.
635 *Journal of Ovarian Research* **8** 24. (doi:10.1186/s13048-015-0151-5)

636 Sander VA, Hapon MB, Sícaro L, Lombardi EP, Jahn GA & Motta AB 2011 Alterations of
637 folliculogenesis in women with polycystic ovary syndrome. *The Journal of Steroid*
638 *Biochemistry and Molecular Biology* **124** 58–64. (doi:10.1016/j.jsbmb.2011.01.008)

639 Silvestris E, de Pergola G, Rosania R & Loverro G 2018 Obesity as disruptor of the female
640 fertility. *Reproductive Biology and Endocrinology: RB&E* **16** 22.
641 (doi:10.1186/s12958-018-0336-z)

642 Singh P, Amin M, Keller E, Simerman A, Aguilera P, Briton-Jones C, Hill DL, Abbott DH,
643 Chazenbalk G & Dumesic DA 2013 A novel approach to quantifying ovarian cell
644 lipid content and lipid accumulation in vitro by confocal microscopy in lean women
645 undergoing ovarian stimulation for in vitro fertilization (IVF). *Journal of Assisted*
646 *Reproduction and Genetics* **30** 733–740. (doi:10.1007/s10815-013-9976-2)

647 Strauss JF 2019 Organization of Ovarian Steroidogenic Cells and Cholesterol Metabolism.
648 In *The Ovary*, pp 83–94. Elsevier. (doi:10.1016/B978-0-12-813209-8.00005-4)

649 Trigatti B, Rayburn H, Viñals M, Braun A, Miettinen H, Penman M, Hertz M, Schrenzel M,
650 Amigo L, Rigotti A *et al.* 1999 Influence of the high density lipoprotein receptor SR-
651 BI on reproductive and cardiovascular pathophysiology. *Proceedings of the*
652 *National Academy of Sciences of the United States of America* **96** 9322–9327.

653 Vélez LM, Abruzzese GA & Motta AB 2013 The biology of the peroxisome proliferator-
654 activated receptor system in the female reproductive tract. *Current*
655 *Pharmaceutical Design* **19** 4641–4646.

Wang L & Menon KMJ 2005 Regulation of Luteinizing Hormone/Chorionic Gonadotropin Receptor Messenger Ribonucleic Acid Expression in the Rat Ovary: Relationship to Cholesterol Metabolism. *Endocrinology* **146** 423–431. (doi:10.1210/en.2004-0805)

Wolf CJ 2002 Effects of Prenatal Testosterone Propionate on the Sexual Development of Male and Female Rats: A Dose-Response Study. *Toxicological Sciences* **65** 71–86. (doi:10.1093/toxsci/65.1.71)

Wu LL-Y, Dunning KR, Yang X, Russell DL, Lane M, Norman RJ & Robker RL 2010 High-fat diet causes lipotoxicity responses in cumulus-oocyte complexes and decreased fertilization rates. *Endocrinology* **151** 5438–5445. (doi:10.1210/en.2010-0551)

Xu N, Taylor KD, Azziz R & Goodarzi MO 2010 Variants in the HMG-CoA Reductase (HMGCR) Gene Influence Component Phenotypes in Polycystic Ovary Syndrome. *Fertility and Sterility* **94** 255-60.e1-2. (doi:10.1016/j.fertnstert.2009.01.158)

Yan X, Yuan C, Zhao N, Cui Y & Liu J 2014 Prenatal androgen excess enhances stimulation of the GNRH pulse in pubertal female rats. *Journal of Endocrinology* **222** 73–85. (doi:10.1530/JOE-14-0021)

Yildirim B, Demir S, Temur I, Erdemir R & Kaleli B 2007 Lipid peroxidation in follicular fluid of women with polycystic ovary syndrome during assisted reproduction cycles. *The Journal of Reproductive Medicine* **52** 722–726.

Zhu XD, Bonet B & Knopp RH 1997 17beta-Estradiol, progesterone, and testosterone inversely modulate low-density lipoprotein oxidation and cytotoxicity in cultured placental trophoblast and macrophages. *American Journal of Obstetrics and Gynecology* **177** 196–209. (doi:10.1016/s0002-9378(97)70462-9)

Figure legends

Figure 1. Effects of prenatal androgen exposure on lipid concentrations in the ovaries of prenatally hyperandrogenized (PH) and control groups. A) Triglycerides, B) Free fatty acids, C) Phospholipids, D) Cholesterol E) Cholesteryl esters. White dots correspond to animals of the control group (n=6), grey dots to the PHiov phenotype (n=6), and black dots to the PHanov phenotype (n=6). The horizontal bar represents the mean. Statistical

analyses were made by ANOVA; different letters mean statistically significant differences (a vs. b, $p<0.05$).

Figure 2. Effects of prenatal androgen exposure on PPARg system in the ovaries of prenatally hyperandrogenized (PH) and control groups. The graphs correspond to A) mRNA abundance of *Pparg* ($p < 0.01$), B) protein levels of PPARg ($p < 0.05$), C) mRNA levels of *Pgc1a* ($p < 0.01$), D) protein levels of PGC1a ($p < 0.05$), and E) Co-immunoprecipitation of PPARg and PGC1a in ovaries of the prenatally hyperandrogenized (PH) and control groups. White dots correspond to animals of the control group, grey dots to the PHiov phenotype, and black dots to the PHanov phenotype. The horizontal bar represents the mean. A sample size of 6 animals per group was used for mRNA and protein analysis and 5 animals per group for CO-IP analysis. Statistical analyses were made by ANOVA; different letters mean statistically significant differences (a vs. b, $p < 0.05$).

Figure 3. Effects of prenatal androgenization on fatty acid and triacylglycerol metabolism. The graphs correspond to A) mRNA abundance of *Srebp1* ($p<0.01$), B) mRNA abundance of *Atgl* ($p<0.01$) of the prenatally hyperandrogenized (PH) and control groups. White dots correspond to animals of the control group (n=6), grey dots to the PHiov phenotype (n=6), and black dots to the PHanov phenotype (n=6). The horizontal bar represents the mean. Statistical analyses were made by ANOVA; different letters mean statistically significant differences (a vs. b, $p<0.05$).

Figure 4. Prenatal androgenization effects on ovarian cholesterol pathway. The graphs correspond to A) mRNA abundance of *Ldl-r* ($p<0.01$), B) mRNA abundance of *Srb1* ($p<0.05$), C) mRNA abundance of *Hmgcr* ($p<0.01$) of the prenatally hyperandrogenized (PH) and control groups. White dots correspond to animals of the control group (n=6), grey dots to the PHiov phenotype (n=6), and black dots to the PHanov phenotype (n=6). The horizontal bar represents the mean. Statistical analyses were made by ANOVA; different letters mean statistically significant differences (a vs. b, $p<0.05$).

Figure 5. Prenatal androgenization effects on ovarian lipid peroxidation.

Lipoperoxidation index using the thiobarbituric acid method (TBARS) through the evaluation of malondialdehyde (MDA) was measured in the prenatally hyperandrogenized (PH) and control groups. White dots correspond to animals of the control group (n=7), grey dots to the PHiov phenotype (n=7), and black dots to the PHanov phenotype (n=7). The horizontal bar represents the mean. Statistical analyses were made by ANOVA; different letters mean statistically significant differences (a vs. b, $p<0.05$).

Figure 6. Prenatal androgen excess effects on ovarian steroidogenic factors and enzymes. Protein expression of A) Steroidogenic acute regulator (StAR), B) 3-B-Hydroxysteriod dehydrogenase (3BHSD), C) cytochrome P450 17a-hydroxylase (CYP17), D) 17β-hydroxysteroid dehydrogenase (17BHSD) and E) cytochrome P450 aromatase (CYP19) in the ovaries of the prenatally hyperandrogenized (PH) and control animals. White dots correspond to animals of the control group (n=6), grey dots to the PHiov phenotype (n=6),

729 and black dots to the PHanov phenotype (n=6). The horizontal bar represents the mean.
730 Statistical analyses were made by ANOVA; different letters mean statistically significant
731 differences (a vs. b, $p<0.05$).

732

733 **Table 1.** List of primers used in real-time PCR. F, forward sequence; R, reverse sequence.

734

735 **Table 2.** List of primary antibodies and dilution used for western blotting.

736

737 **Table 3.** Metabolic and hormonal parameters at adulthood for the prenatally
738 hyperandrogenized (PH) and control groups for 7 rats per group. Values represent mean ±
739 S.D. Statistical analyses were made by ANOVA with post hoc Tukey's test. Different letters
740 mean statistically significant differences (a vs. b, $p<0.05$).

741

Table 1. List of primers used in Real-time PCR

Primers used in Real-time PCR		
Gene	**Primers sequences**	**Temperature of annealing (ºC)**
Atgl F	AACCATCATTCTCGGCTCAC	62
Atgl R	CCCACCAGGAGTAGCATTGT	
Hmgcr F	TGCTGCTTTGGCTGTATGTC	62
Hmgcr R	TGAGCGTGAACAAGAACCAG	
L32 F	TGGTCCACAATGTCAAGG	58
L32 R	CAAAACAGGCACACAAGC	
Ldl-r F	AGACCCAGAGCCATCGTAGT	62
Ldl-r R	ATCAACCCAATAGAGGCGGC	
Pgc1a F	AATGCAGCGGTCTTAGCACT	60
Pgc1a R	GTGTGAGGAGGGTCATCGTT	
***Pparg* F**	TTTTCAAGGGTGCCAGTTTC	60
***Pparg* R**	GAGGCCAGCATGGTGTAGAT	
Psmb2 F	TCGGAGTCGGACCCCTTATC	62
Psmb2 R	TGTAGTAAAGTGCTGGCCCC	
Srb1 F	GGTGCCCATCATTTACCAAC	62
Srb1 R	CCCTACAGCTTGGCTTCTTG	
Srebp F	TAACCTGGCTGAGTGTGCAG	60
Srebp R	ATCCACGAAGAAACGGTGAC	

F, forward sequence; R, reverse sequence

Table 2. List of primary antibodies and dilution used for western blotting.

Antibody	Brand	Catalogue number	Western blot dilution
PPARg	ABCAM	ab19481	1:200
PGC1a	Santa Cruz Biotechnology	sc13067	1:200
StAR	Santa Cruz Biotechnology	sc25806	1:200
3BHSD	Santa Cruz Biotechnology	sc28206	1:200
17BHSD	Santa Cruz Biotechnology	Sc32872	1:200
CYP17	Santa Cruz Biotechnology	Sc66849	1:200
CYP19	Santa Cruz Biotechnology	Sc30086	1:200

Table 3. Metabolic and hormonal characterization at adulthood.

Parameter	Control	PHiov	PHanov
Body weight at 90 days of age (g)	228.33 ± 19.03[a]	225.22 ± 21.27[a]	229.89 ± 26.78[a]
Average Ovarian Weight (mg)	46.3 ± 10.44[a]	46.82 ± 8.77[a]	36.58 ± 4.75[b]
Total Cholesterol (mg/dL)	132.03 ± 23.75[a]	136.78 ± 39.69[a]	128.94 ± 35.97[a]
HDL Cholesterol (mg/dL)	31.72 ± 4.49[a]	28.53 ± 5.83[a]	32.16 ± 5.06[a]
LDL Cholesterol (mg/dL)	58.44 ± 21.99[a]	105.20 ± 28.37[b]	97.20 ± 38.17[b]
Triglycerides (mg/dL)	86.08 ± 31.89[a]	119.00 ± 24.59[b]	112.42 ± 12.03[b]
LH (ng/mL)	0.31 ±0.05[a]	0.61 ± 0.29[a]	0.45 ± 0.34[a]
FSH (ng/mL)	3.54 ± 2.06[a]	3.43 ± 1.29[a]	4.23 ± 2.61[a]
Progesterone (ng/mL)	8.16 ± 5.52[a]	17.16 ± 9.72[a]	12.86 ± 9.6[a]
Testosterone (pg/mL)	75.05 ± 18.29[a]	93.59 ± 17.26[a]	213.23 ± 11.00[b]
Estradiol (pg/mL)	14.28 ± 4.66[a]	7.69 ± 3.19[b]	7.34 ± 2.56[b]

Metabolic and hormonal parameters for the prenatally hyperandrogenized (PH) and Control groups for 7 rats per group. Values represent mean ± S.D. Statistical analyses were made by ANOVA with post hoc Tukey's test. Different letters mean statistically significant differences (a vs. b, $p<0.05$).

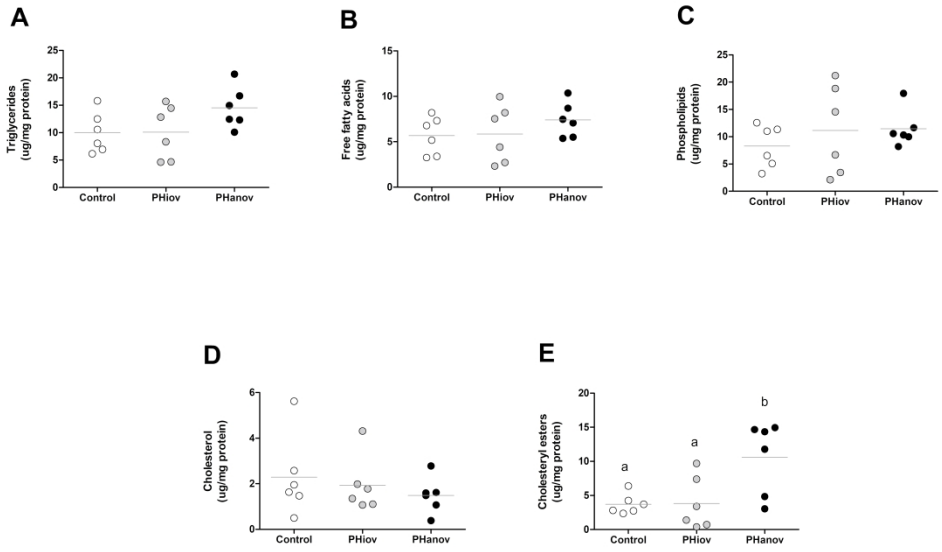

Figure 1. Effects of prenatal androgen exposure on lipid concentrations in the ovaries of prenatally hyperandrogenized (PH) and control groups. A) Triglycerides, B) Free fatty acids, C) Phospholipids, D) Cholesterol E) Cholesteryl esters. White dots correspond to animals of the control group (n=6), grey dots to the PHiov phenotype (n=6), and black dots to the PHanov phenotype (n=6). The horizontal bar represents the mean. Statistical analyses were made by ANOVA; different letters mean statistically significant differences (a vs. b, $p<0.05$).

150x87mm (1200 x 1200 DPI)

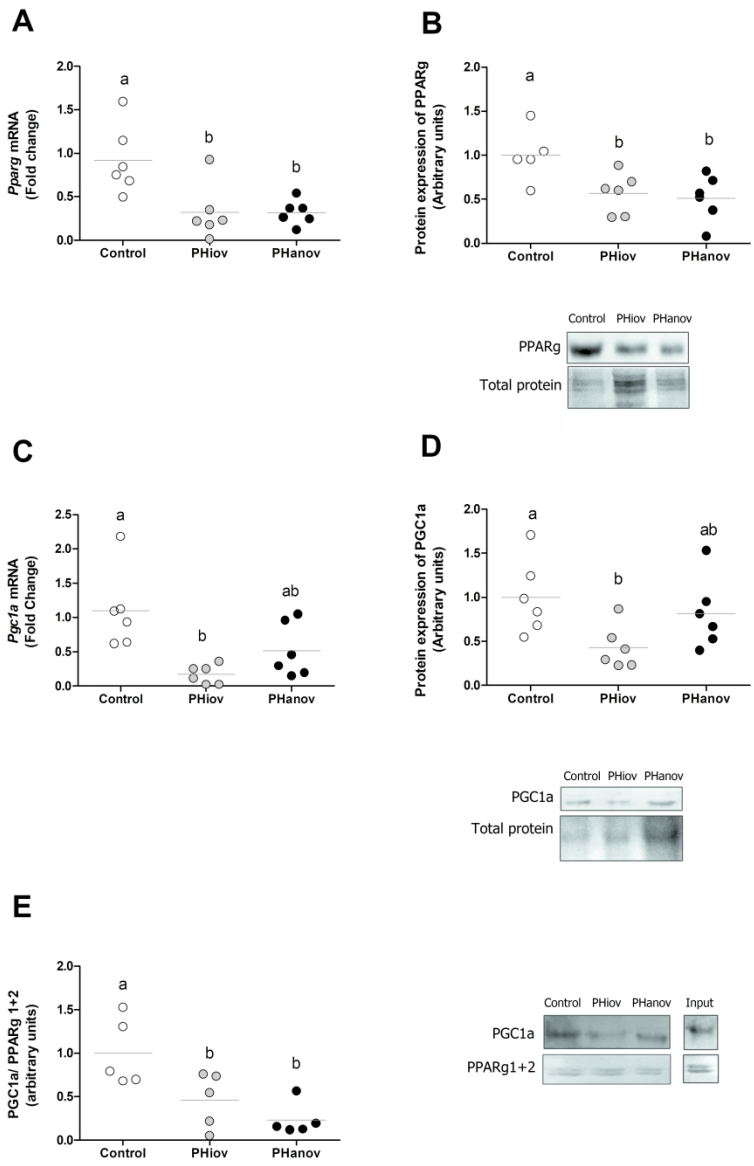

Figure 2. Effects of prenatal androgen exposure on PPARg system in the ovaries of prenatally hyperandrogenized (PH) and control groups. The graphs correspond to A) mRNA abundance of Pparg ($p < 0.01$), B) protein levels of PPARg ($p < 0.05$), C) mRNA levels of Pgc1a ($p < 0.01$), D) protein levels of PGC1a ($p < 0.05$), and E) Co-immunoprecipitation of PPARg and PGC1a in ovaries of the prenatally hyperandrogenized (PH) and control groups. White dots correspond to animals of the control group, grey dots to the PHiov phenotype, and black dots to the PHanov phenotype. The horizontal bar represents the mean. A sample size of 6 animals per group was used for mRNA and protein analysis and 5 animals per group for CO-IP analysis. Statistical analyses were made by ANOVA; different letters mean statistically significant differences (a vs. b, $p < 0.05$).

100x144mm (1200 x 1200 DPI)

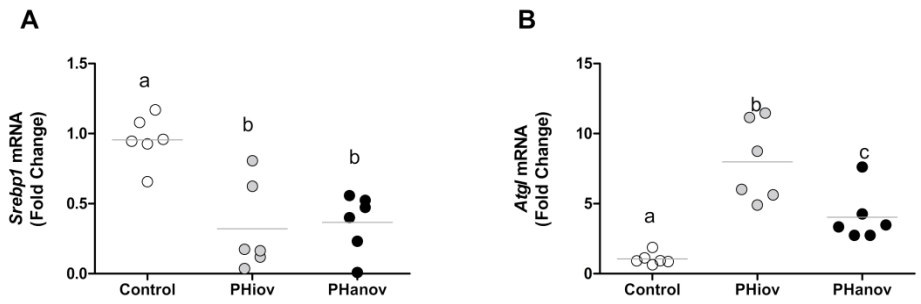

Figure 3. Effects of prenatal androgenization on fatty acid and triacylglycerol metabolism. The graphs correspond to A) mRNA abundance of Srebp1 ($p<0.01$), B) mRNA abundance of Atgl ($p<0.01$) of the prenatally hyperandrogenized (PH) and control groups. White dots correspond to animals of the control group (n=6), grey dots to the PHiov phenotype (n=6), and black dots to the PHanov phenotype (n=6). The horizontal bar represents the mean. Statistical analyses were made by ANOVA; different letters mean statistically significant differences (a vs. b, $p<0.05$).

99x33mm (1200 x 1200 DPI)

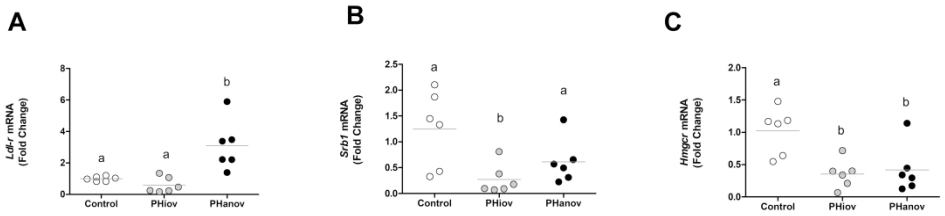

Figure 4. Prenatal androgenization effects on ovarian cholesterol pathway. The graphs correspond to A) mRNA abundance of Ldl-r ($p<0.01$), B) mRNA abundance of Srb1 ($p<0.05$), C) mRNA abundance of Hmgcr ($p<0.01$) of the prenatally hyperandrogenized (PH) and control groups. White dots correspond to animals of the control group (n=6), grey dots to the PHiov phenotype (n=6), and black dots to the PHanov phenotype (n=6). The horizontal bar represents the mean. Statistical analyses were made by ANOVA; different letters mean statistically significant differences (a vs. b, $p<0.05$).

99x24mm (1200 x 1200 DPI)

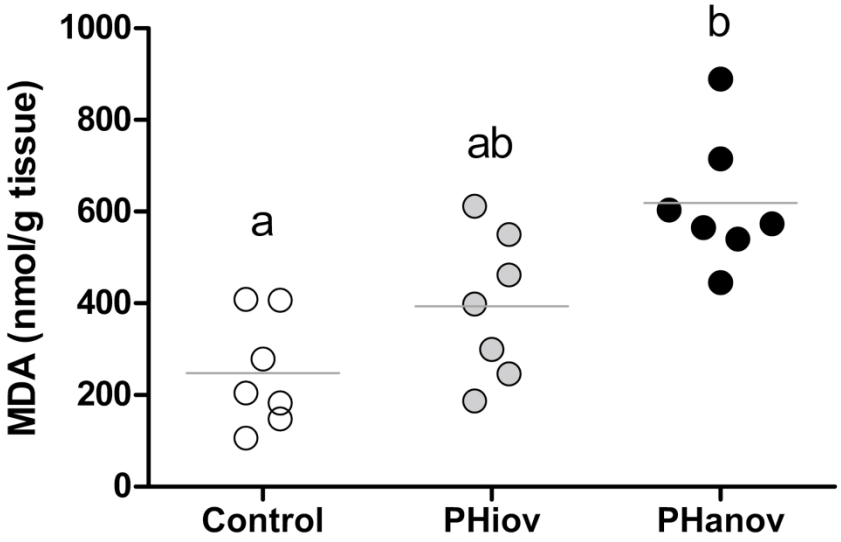

Figure 5. Prenatal androgenization effects on ovarian lipid peroxidation.
Lipoperoxidation index using the thiobarbituric acid method (TBARS) through the evaluation of malondialdehyde (MDA) was measured in the prenatally hyperandrogenized (PH) and control groups. White dots correspond to animals of the control group (n=7), grey dots to the PHiov phenotype (n=7), and black dots to the PHanov phenotype (n=7). The horizontal bar represents the mean. Statistical analyses were made by ANOVA; different letters mean statistically significant differences (a vs. b, $p<0.05$).

49x31mm (1200 x 1200 DPI)

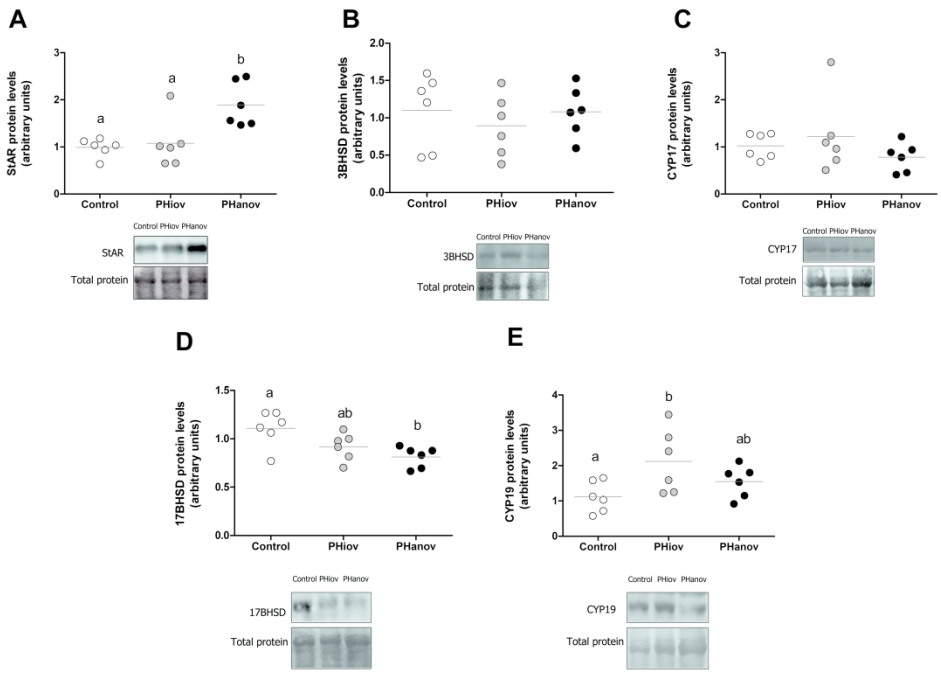

Figure 6. Prenatal androgen excess effects on ovarian steroidogenic factors and enzymes. Protein expression of A) Steroidogenic acute regulator (StAR), B) 3-B-Hydroxysteriod dehydrogenase (3BHSD), C) cytochrome P450 17a-hydroxylase (CYP17), D) 17β-hydroxysteroid dehydrogenase (17BHSD) and E) cytochrome P450 aromatase (CYP19) in the ovaries of the prenatally hyperandrogenized (PH) and control animals. White dots correspond to animals of the control group (n=6), grey dots to the PHiov phenotype (n=6), and black dots to the PHanov phenotype (n=6). The horizontal bar represents the mean. Statistical analyses were made by ANOVA; different letters mean statistically significant differences (a vs. b, $p<0.05$).